

Interaction between massive planets on inclined orbits and circumstellar discs

M. Xiang-Gruess¹ * and J. C. B. Papaloizou¹

¹ *Department of Applied Mathematics and Theoretical Physics, University of Cambridge, Wilberforce Road, Cambridge CB3 0WA, United Kingdom*

Accepted . Received ;

ABSTRACT

We study the interaction between massive planets and a gas disc with a mass in the range expected for protoplanetary discs. We use SPH simulations to study the orbital evolution of a massive planet as well as the dynamical response of the disc for planet masses between 1 and 6 M_J and the full range of initial relative orbital inclinations.

We find that gap formation can occur for planets in inclined orbits as well as for coplanar orbits as expected. For given planet mass, a threshold relative orbital inclination exists under which a gap forms. This threshold increases with planet mass. Orbital migration manifest through a decreasing semi-major axis is seen in all cases.

At high relative inclinations, the inclination decay rate increases for increasing planet mass and decreasing initial relative inclination as is expected from estimates based on dynamical friction between planet and disc. For an initial semi-major axis of 5 AU and relative inclination of $i_0 = 80^\circ$, the times required for the inclination to decay by 10° is $\sim 10^6$ yr and $\sim 10^5$ yr for 1 M_J and 6 M_J respectively, these times scaling in the usual way for larger initial orbits. For retrograde planets, the inclination always evolves towards coplanarity with the disc, with the rate of evolution being fastest for orbits with $i_0 \rightarrow 180^\circ$. The indication is thus that, without taking account of subsequent operation of phenomena such as the Lidov-Kozai effect, planets with mass 1 M_J initiated in circular orbits with semi-major axis ~ 5 AU and $i_0 \sim 90^\circ$ might only just become coplanar, as a result of frictional effects, within the disc lifetime. In other cases highly inclined orbits will survive only if they are formed after the disc has mostly dispersed.

Planets on inclined orbits warp the disc by an extent that is negligible for 1 M_J but increases with increasing mass becoming quite significant for a planet of mass 6 M_J . In that case, the disc can gain a total inclination of up to 15° together with a warped inner structure with an inclination of up to $\sim 20^\circ$ relative to the outer part. We also find a solid body precession of both the total disc angular momentum vector and the planet orbital momentum vector about the total angular momentum vector, with the angular velocity of precession decreasing with increasing relative inclination as expected in that case.

Our results illustrate that the influence of an inclined massive planet on a protoplanetary disc can lead to significant changes of the disc structure and orientation which can in turn affect the orbital evolution of the planet significantly. A three-dimensional treatment of the disc is then essential in order to capture all relevant dynamical processes in the composite system.

Key words: planetary systems: formation – planetary systems: protoplanetary discs – planetary systems: planet-disc interactions

1 INTRODUCTION

In the past few decades, the number of detected extrasolar planets around other main sequence stars has increased dramatically, so that at the time of writing, more than 840

* E-mail: mx216@cam.ac.uk

planets have been discovered. Well studied planet formation scenarios such as core accretion (Mizuno 1980; Pollack et al. 1996) or disc fragmentation (Mayer et al. 2002) involve the planet forming in a disc with the natural expectation that the orbit should be coplanar. However, Rossiter McLaughlin measurements of close orbiting hot Jupiters indicate that around 40% have angular momentum vectors significantly misaligned with the angular velocity vector of the central star (e.g. Triaud et al. 2010; Albrecht et al. 2012). As the stellar and disc angular velocities are naturally expected to be aligned, this would imply an inclination of the planet orbit relative to the nascent protoplanetary disc. But note that (e.g. Lai et al. 2011) have proposed that a magnetic interaction between the central star and protoplanetary disc could lead to the stellar angular momentum vector being misaligned with that of the disc, in which case misaligned planetary orbits need not be inferred. However, Watson et al. (2011) have compared stellar rotation axis inclination angles with measured debris-disc inclinations and found no evidence for misalignment.

Several scenarios have been proposed to explain the origin of misalignments between the planetary orbital angular momentum vector and the stellar rotation axis for close in planets. The first involves excitation of very high eccentricities, either through the Lidov-Kozai effect induced by the interaction with a distant companion (e.g. Fabrycky & Tremaine 2007; Wu et al. 2007), or through planet-planet scattering or chaotic interactions (e.g. Weidenschilling & Marzari 1996; Rasio & Ford 1996; Papaloizou & Terquem 2001; Nagasawa et al. 2008). This is then followed by orbital circularization due to interaction with the central star, although aspects of this process are not yet understood in detail (Dawson et al. 2012). It is possible that high eccentricities and inclinations for massive planets are generated when the disc is present. It is then important, as has been noted by Dawson et al. (2012), to understand the interactions with the disc and consequent time scales for realignment.

Another method for producing high inclinations has been indicated by Thommes & Lissauer (2003), who have studied the evolution of two giant planets in resonance, with an approximate analytical expression for the influence of a gas disc in producing orbital migration. Their calculations suggest that resonant inclination excitation can occur when through the interaction between the planets the eccentricity of the inner planet reaches a threshold value of $e_1 \geq 0.6$. Inclinations gained by the resonant pair of planets can reach values up to $\sim 60^\circ$. The effects of disc planet interactions may be significant here also.

Another explanation for the origin of misaligned planets is connected with the possibility that the orientation of the disc changes, possibly due to lack of alignment of the source material or due to gravitational encounters with passing stars, either before or after the planet forms (e.g. Bate et al. 2010; Thies et al. 2011). However, up to now, there is no observational evidence for such disc misalignment (Watson et al. 2011).

While the formation of planets on misaligned orbits has been a frequent topic of debate, the evolution of massive planets on misaligned orbits interacting with a disc is still not well understood. Many hydrodynamical simulations have been performed in order to study the influence of a pro-

toplanetary disc on the evolution of planets. The majority of these simulations have considered planets that are coplanar with the disc and been two dimensional and used grid-based methods (see Papaloizou et al. 2007; Kley & Nelson 2012, for a review and references therein).

Planets with initial orbital inclinations with respect to a disc have been studied (e.g. Cresswell et al. 2007; Bitsch & Kley 2011). In these works the evolution of planets with masses up to a maximum of $1M_J$ with different initial eccentricities and relatively small initial inclinations up to a maximum of 15° interacting with three-dimensional isothermal and radiative discs are considered. They showed damping for both eccentricity and inclination with the planets circularising in the disc after a few hundred orbits.

In this paper we are interested in extending studies of disc planet interactions involving planets with orbital planes misaligned with that of the disc to consider larger planet masses of up to several Jupiter masses and the full range of inclinations. In such cases the interaction with the disc is more likely to be described by dynamical friction than being the result of the application of resonant torques that is applicable in the coplanar case (see for example Papaloizou & Larwood 2000; Rein 2012; Teyssandier et al. 2013). Numerical simulations of warped discs in close binary systems were performed by e.g. Larwood et al. (1996); Fragner & Nelson (2010). These works indicate that thick discs with low viscosities have efficient warp communication which allows them to precess as rigid bodies with little warping or twisting while thinner discs can develop twists before reaching a state of rigid-body precession. Possible warping of a disc by giant planets has yet to be studied in detail. It has been estimated from linearized calculations (Teyssandier et al. 2013) that disc warping should be a small effect for sub Jovian mass planets, this being confirmed by the results of this paper. However, it turns out to be significant for larger planet masses that can produce significant nonlinear effects, therefore we study these effects in this paper.

It has been shown that Smoothed particle hydrodynamics (SPH) simulations are capable of being applied to the problem of planet-disc interaction (e.g. Schäfer et al. 2004; de Val-Borro et al. 2006) though in comparison to grid-based simulation methods, they incur greater computational expense. But in contrast to grid-based methods, as they adopt a Lagrangian approach, SPH simulations can be readily used to simulate a gas disc with a free boundary in three dimensions with the disc having the freedom to change its shape at will, thus we adopt this approach here. Similarly, Marzari & Nelson (2009) studied the interaction between a Jupiter mass planet and a disc using the SPH method. Initial eccentricities ranging from 0 to 0.4 and an initial inclination of 20° were considered. The disc is simulated by the SPH code VINE that is similar to GADGET-2 and a locally isothermal equation of state. They find that both the eccentricity and the inclination are damped on a timescale much lower than the disc lifetime ($\sim 10^6$ yr).

In this paper we consider a range of planet masses and the full range of orbital inclinations. In addition to studying the warping response of the disc, we estimate the timescales for orbital evolution and attainment of coplanarity. We also make a preliminary study of the potential exchange of inclination and eccentricity that might be expected for high

inclination orbits through the operation of an adaption of the Lidov-Kozai mechanism. The plan of the paper is as follows:

In Section 2, we describe our simulation code with a description of the modified locally isothermal equation of state we adopted (Section 2.1). Some details concerning the smoothing length and artificial viscosity are given in Section 2.2. In Section 3, we describe the general setup for the disc, planet and the central star. In Section 4, we give a brief overview of the interaction between a massive planet and disc. We give an analytic estimate of the evolution time scale for a planet interacting with a disc based on considerations of dynamical friction, in order to compare with our simulations, in Section 4.2. In addition, we consider the possibility of the Lidov-Kozai effect (Section 4.3). In Section 5, we discuss numerical results for a massive planet on a coplanar circular orbit. We study the evolution of planets initiated on inclined orbits in Section 6 considering the evolution of both initially prograde and retrograde circular orbits. In Section 7, we study disc warping and precession. In Section 8, we study a planet starting on an eccentric inclined orbit finding evidence for some exchange of inclination and eccentricity as might be expected from a Lidov-Kozai like process. The behaviour of an inclined planet interacting with discs of different masses is considered in Section 8.1. Finally the results are summarised and discussed in Section 9.

2 SIMULATION DETAILS

We have performed simulations using a modified version of the publically available code GADGET-2 (Springel 2005). GADGET-2 is a hybrid N-body/SPH code capable of modelling both fluid and distinct fixed or orbiting massive bodies. In our case the central star, of mass M_* , is fixed and the planet, of mass M_p , orbits as a distinct massive body. We adopt spherical polar coordinates (r, θ, ϕ) with origin at the centre of mass of the central star.

The gaseous disc is represented by SPH particles. An important issue in N-body/SPH simulations is the choice of the gravitational softening lengths. Ideally, gravitational force computations without softening should be used to determine the gravitational interactions between particles. However, for numerical reasons, a softening length has to be introduced. This is because SPH particles would experience very high gravitational accelerations in the vicinity of massive objects. In turn, this would result in unacceptably small time steps that prevent simulations from effectively proceeding. For this reason, we adopt gravitational softening lengths that are sufficiently large to enable the calculation to proceed, and in the case of the planet, smaller than physically relevant length scales such as the disc height H and the planetary Hill radius. It can be associated with a physical size of material considered to be bound to the planet. Here we study planets of masses $M_p \geq 1 M_J$ with an orbital length scale of $R_p = 5$ AU and discs with aspect ratio $H/r = 0.05$. Thus the Hill radius defined as $R_H = R_p (M_p / (3M_*))^{1/3}$ is 0.35 AU for a Jupitermass planet at 5 AU. At $r = 5$ AU, $H = 0.25$ AU. In our simulations, the central star and the planet are unsoftened when interacting with each other allowing them to undergo close encounters accurately, although they do not actually occur in our simulations. For

the computation of the gravitational interaction between the massive bodies and the SPH particles, we adopted fixed softening lengths $\varepsilon_* = 0.4$ AU and $\varepsilon_p = 0.1$ AU for the central star and the planet, respectively. The former value controls conditions near the central star. These are not significant for the dynamics of interest in our simulations which only depend on the value of the central stellar mass. The latter value ε_p controls conditions close to the planet and is significantly smaller than both $R_H(1 M_J, 5 \text{ AU})$ and $H(5 \text{ AU})$.

The star and the planet are allowed to accrete gas particles that approach them very closely. The reason for doing this is to prevent the possibility of strong unresolved forces occurring close to massive objects. In this respect it works in tandem with softening. In order to implement accretion, we followed the procedure of Bate et al. (1995) for so-called "sink particles". This was applied such that for the star and planet, the outer accretion radii were fixed during the simulation to be $R_{acc,*} = 7 \times 10^{11}$ cm and $R_{acc,p} = 7 \times 10^{10}$ cm respectively. SPH particles that come within the accretion radius of a sink particle, are accreted if they fulfill all conditions for accretion. Firstly, the particle must be bound to the sink particle. Secondly, its specific angular momentum about the sink particle must be less than that required for it to form a circular orbit at R_{acc} about the sink particle. These conditions ensure that particles which would normally leave the accretion radius are not accreted. Thirdly, the particle must be more tightly bound to the candidate sink particle than to any other sink particle. In our case this is to allow for the possibility that, given the very different masses of the star and planet, a SPH particle could pass through the accretion radius of the planet and yet be accreted by the central star.

An inner accretion radius can also be defined such that SPH particles are accreted regardless of the tests (Bate et al. 1995). By using an inner accretion radius, particles are prevented from being accelerated by very close encounters with the sink particle that might otherwise dramatically slow down the simulation. Bate et al. (1995) suggests that the inner accretion radius should be 10-100 times smaller than the outer accretion radius. Due to our very small outer accretion radii, the choice of the inner accretion radii to be 0.5 R_{acc} was found to be adequate for this purpose.

In practice, for the equations of state and softening parameters we used for most of our simulations, because of the relatively small accretion radii adopted, the accretion of gas particles was found to play only a minor role, producing negligible changes to the masses of the planet and star (see also the discussion in section 5.1).

2.1 Equation of state

For the hydrodynamical simulations, we applied a locally isothermal equation of state with the modification described by Peplinski et al. (2008). The reason for modification is because, as Peplinski et al. (2008) have pointed out, if the temperature characteristic of the main disc is adopted in the vicinity of the planets, a high concentration of gas leading to rapid accretion develops in the close vicinity of massive planets. Accordingly, we adopt a sound speed given by

(Peplinski et al. 2008)

$$c_s = \frac{h_s r_s h_p r_p}{[(h_s r_s)^n + (h_p r_p)^n]^{1/n}} \sqrt{\Omega_s^2 + \Omega_p^2}, \quad (1)$$

Here $r_s = |\mathbf{r} - \mathbf{r}_s|$ and $r_p = |\mathbf{r} - \mathbf{r}_p|$ are the distances to the central star and the planet respectively, and Ω_s and Ω_p are the angular velocities in the circumstellar and circumplanetary discs. For pure Keplerian motion they are given by

$$\Omega_s = \sqrt{\frac{GM_*}{r_s^3}} \quad \text{and} \quad \Omega_p = \sqrt{\frac{GM_p}{r_p^3}} \quad \text{respectively.} \quad (2)$$

The disc aspect ratio is $h_s = H/r_s$ with H being the disc scale height. The parameter n was taken to be $n = 3.5$. For the simulations we take $H/r_s = c_s/v_\varphi = 0.05$, where $v_\varphi = r_s \Omega_s$ is the rotational velocity. As $r_p \rightarrow 0$, the sound speed in the circumplanetary disc is $h_p r_p \Omega_p$ and accordingly h_p is the aspect ratio in that limit. This should be chosen large enough so that pressure forces prevent excessive gas accumulation on the planet. At the same time, it must be chosen large enough to prevent values of the sound speed that are smaller than the unmodified value, at locations that are a moderate distance away from the planet. Peplinski et al. (2008) suggest $h_p \geq 0.4$. A discussion of the effects resulting from different choices of h_p can be found in appendix A. For our simulations, we adopted $h_p = 0.6$ which was large enough to prevent unrealistically fast gas accretion while not causing the sound speed to become smaller than the unmodified value in all cases.

2.2 Smoothing length and artificial viscosity

For our SPH calculations, the smoothing length was adjusted so that the number of nearest neighbours to any particle contained within a sphere of radius equal to the local smoothing length was 40 ± 5 . The pressure is given by $p = \rho c_s^2$. Thus apart from the vicinity of the planet, the temperature in the disc is $\propto r^{-1}$. The artificial viscosity parameter α of GADGET-2 (see equations (9) and (14) of Springel 2005) was taken to be $\alpha = 0.5$.

The artificial viscosity is modified by the application of a viscosity-limiter to reduce artificially induced angular momentum transport in the presence of shear flows. This is especially important for the study of Keplerian discs. In order to calibrate the diffusive effects resulting from this viscosity, we applied the ring spreading test to determine an effective kinematic viscosity measured through the α_{SS} parameter (Shakura & Sunyaev 1973). Details are given in appendix B. A value of $\alpha = 0.5$, showed the best match to the analytic ring spreading solution with $\alpha_{SS} = 0.02$ and was hence used in all simulations. SPH simulations accordingly model a viscous disc, with a viscosity that behaves like a conventional Navier Stokes viscosity in this context. It should be noted that the effective viscosity in protoplanetary discs is likely to involve magnetic fields and behave differently in some contexts. However many of the simulations undertaken here involve impulsive high velocity interactions between planet and disc that are characteristically described by dynamical friction (see below) and for which the disc viscosity is not expected to play a major role. The remaining simulations involve coplanar, inwardly migrating,

gap forming planets for which the interaction with the disc is nonlinear and long range. The characteristic behaviour again is not expected to be sensitive to details of the viscosity (e. g. Nelson & Papaloizou 2003; Baruteau et al. 2011).

3 INITIAL CONDITIONS

We study a system composed of a central star of one solar mass M_\odot , a gaseous disc and a massive planet. The disc is set up such that the angular momentum vector for all particles was in the same direction enabling a mid plane for the disc to be defined. Planet masses in the range 1 - 6 M_J were initiated in circular orbits with inclinations in the range $i_0 = [0; 80]^\circ$ with respect to the initial disc mid plane. The semi-major axis of the planet was set to $a = 5$ AU. The particle distribution was chosen to model a surface density profile such that

$$\Sigma = \Sigma_0 R^{-1/2}. \quad (3)$$

Here Σ_0 is a constant and R is the radial coordinate of a point in the midplane, here taken to occupy the radial domain $[0, R_{out} - \delta]$, with $R_{out} = 5a$ and $\delta = 0.4a$. A taper was applied such that the surface density was set to decrease linearly to zero for R in the interval $[R_{out} - \delta, R_{out} + \delta]$. The total disc radial domain is hence $[0, R_{out} + \delta]$.

The disc mass is given by

$$M_D = 2\pi \int_0^{R_{out}} \Sigma(r) r dr = \frac{4}{3} \pi \Sigma_0 R_{out}^{3/2} r, \quad (4)$$

which is used to determine Σ_0 . The disc particles were set up in a state of pure Keplerian rotation velocity according to

$$v_\varphi = \sqrt{r_s \frac{d\Phi_*}{dr_s}}. \quad (5)$$

The radial velocities were set to be zero. Here Φ_* is the gravitational potential due to the central star. In the innermost region around the central star, the disc properties (e.g. Ω_s and accordingly c_s) are modified by the softening.

In this paper, only discs for which self-gravity can be neglected are studied. For this to be possible with a locally isothermal equation of state, the Toomre parameter has to fulfil the requirement

$$Q = \frac{\Omega c_s}{\pi G \Sigma} > 1.4. \quad (6)$$

For the case $H/r_s = 0.05$, the Toomre parameter can be expressed as

$$Q = \frac{0.05 M_*}{r_s^2 \pi \Sigma} = \frac{R_{out}^{3/2} M_*}{15 M_D} r_s^{-3/2}. \quad (7)$$

For a disc with any arbitrary outer radius R_{out} , the maximum allowed disc mass $M_{D,max}$, which fulfils the requirement that $Q(R_{out}) = 1.4$ at its outer edge is

$$M_{D,max} = \frac{M_*}{15Q(R_{out})} = \frac{M_*}{21}. \quad (8)$$

Hence, for any arbitrarily chosen outer radius R_{out} , the total disc mass has to be set smaller than $M_*/21 \sim 0.05 M_*$. For simulations shown in this paper, the disc mass is $M_D =$

0.01 M_\odot unless stated otherwise which corresponds to

$$\Sigma_0 = \frac{3M_D}{4\pi R_{out}^{3/2}} = \frac{0.03 M_\odot}{20\sqrt{5}\pi a^{3/2}}. \quad (9)$$

The disc mass surface density at the location of a planet with $a = 5$ AU is then 76 g cm^{-2} .

In addition to self-gravity, energy transfer and mass in-fall onto the disc are neglected. At the start of a simulation, the disc is allowed to evolve for 30 orbits before the planet is introduced. By doing this, we minimise the effects of initial transients in the disc arising from the setup.

In order to examine the effect of changing the number of SPH particles, we performed resolution studies with both coplanar planets and planets initiated on inclined orbits. These are described in appendix C. The number of SPH particles chosen for most of our simulations was 2×10^5 . This enabled enough simulations to be run for ~ 500 orbits or $500 \times P(5 \text{ AU}) = 500 \times 11.18 \text{ yr} = 5600 \text{ yr}$ that a reasonable exploration of phase space could be made while retaining adequate accuracy. Finally we note that although for definiteness we have fixed length and time units to correspond to 5 AU, they can be scaled to other values with the usual corresponding scaling of the units of length and time.

4 ORBITAL EVOLUTION OF A SINGLE MASSIVE PLANET

4.1 General overview

The evolution of a system composed of a central star, a planet and a gaseous disc is dependent on the relative masses of the different components. Low-mass planets produce relatively small amplitude density perturbations such that the global disc evolution is not significantly modified. In contrast, a massive planet can influence the global evolution of a disc significantly in two ways. Firstly, material may be cleared from its neighbourhood by tidal interaction, creating a deep and wide gap. Secondly, it is expected that massive planets on inclined orbits could modify the three-dimensional structure of the disc by producing large scale twists and warps. However, this has not yet been studied in detail.

In the mass domain $M_p \in [1M_J; 6M_J]$ considered here, a planet in a coplanar orbit is expected and been found to open a gap in the disc. (e.g. Lin & Papaloizou 1979; Varnière et al. 2004; Crida et al. 2006). In addition net torques acting on the planet result in planet migration. When a planet opens a gap in its host disc, provided it is not too massive, it migrates inward on the viscous timescale of the disc (type II migration).

When the orbit of the planet is significantly inclined with respect to the disc mid plane, the interaction with the disc is expected to differ from the coplanar case. Impulsive interactions occurring twice per orbit that can be described through an approach based on dynamical friction are expected. Recently, Rein (2012) made a local study of low-mass planets on highly inclined orbits and was able to confirm the dynamical friction viewpoint and show that the time-scale for realignment in such cases was long compared to the disc lifetime meaning that such inclined orbits should survive the presence of a disc. For massive planets, the interaction is expected to be stronger with the evolutionary

time scales correspondingly reduced. In addition, the planet is more likely to affect the structure and evolution of the disc.

4.2 Estimate of time scale for orbital evolution

Here we estimate an approximate time scale for orbital evolution assuming that the interaction between the planet and the disc can be described as occurring through dynamical friction. It has been noted by a number of authors (e.g. Papaloizou & Larwood 2000; Rein 2012; Teyssandier et al. 2013) that planets on orbits with high eccentricity and/or high inclination pass through the disc with a high supersonic relative velocity such that the interaction can be approximated as being with pressure-less ballistic fluid particles. A dynamical friction calculation is then appropriate. The frictional force per unit mass is then (e.g. Ruderhmann & Spiegel 1971; Rephaeli & Salpeter 1980; Ostriker 1999)

$$\mathbf{f}_D = -\frac{4\pi G^2 M_p \rho \mathbf{v}_{rel}}{|\mathbf{v}_{rel}|^3} \ln(r_1/r_2), \quad (10)$$

where \mathbf{v}_{rel} is the relative velocity between the planet and disc gas of density ρ . Here r_1 and r_2 represent upper and lower cut off length scales outside of which the analysis leading to (10) that assumes a homogeneous medium becomes invalid. There is some uncertainty in estimating these that in turn leads to an uncertainty in the force of a factor of a few, and so we can only use (10) to make rough estimates. We consider a high inclination orbit and a thin disc such that the interaction may be viewed as impulsive and occurring twice per orbit. Each impulse produces a small velocity change given by

$$\Delta \mathbf{v} = -\frac{4\pi G^2 M_p \ln(r_1/r_2)}{\sin i} \int \frac{\rho \mathbf{v}_{rel}}{|\mathbf{v}_{rel}|^3 |\mathbf{v}|} dz, \quad (11)$$

where the disc mid plane is assumed to lie in a Cartesian (x, y) plane, the inclination of the orbit to the disc is i , the orbital speed is $|\mathbf{v}|$, and the integration is taken through the vertical extent of the disc. For a thin disc this becomes

$$\Delta \mathbf{v} = -\frac{4\pi G^2 M_p \ln(r_1/r_2) \Sigma \mathbf{v}_{rel}}{|\mathbf{v}_{rel}|^3 |\mathbf{v}| \sin i}, \quad (12)$$

where Σ is the disc surface density. This in turn leads to a characteristic time for the orbit to change measured in units of the orbital period given by

$$T_D = |\mathbf{v}_{rel}| / (2|\Delta \mathbf{v}|) = \frac{|\mathbf{v}|^4 \sin i \sin^3(i/2)}{\pi G^2 M_p \ln(r_1/r_2) \Sigma}, \quad (13)$$

where in order to obtain estimates, we have replaced $|\mathbf{v}_{rel}|$ by $2|\mathbf{v}| \sin(i/2)$. To proceed further we set $r = a$, $|\mathbf{v}|^4 = G^2 M_*^2 / a^2$ and $\Sigma = 3M_D(a/R_{out})^{3/2} / (4\pi a^2)$. Thus, we obtain

$$T_D = \frac{M_*^2 \sin i \sin^3(i/2)}{\pi \Sigma M_p a^2 \ln(r_1/r_2)} \equiv \frac{4M_*^2 \sin i \sin^3(i/2)}{3M_p M_D \ln(r_1/r_2)} \left(\frac{R_{out}}{a}\right)^{3/2} \quad (14)$$

In order to estimate r_1 , we note that when the planet is in the disc, the vertical scale should be limited by H , but that r_1 should be somewhat larger to account for more distant material near the disc midplane. Accordingly we take $r_1 = 2H$. For r_2 we take the softening length which is around $0.4H$ at $a = 5$ AU. This is an estimate of the scale below which material should be regarded as being bound to the

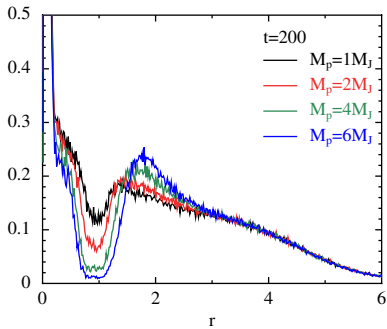


Figure 1. The azimuthally averaged disc surface density profile (in units of $M_J/(5 \text{ AU})^2$) as a function of distance (in units of 5 AU) after 200 hundred orbits for planets with $M_p = 1, 2, 4,$ and $6 M_J$. The curves plotted are such that the density minimum in the centre of the gap decreases with increasing planet mass. [All gap profiles were created using SPLASH (Price 2007)]

planet. Taking $M_D/M_* = 0.01$, $M_p/M_* = 0.001$, $r_1/r_2 = 5$, $R_{out}/a = 5$ and $i = \pi/4$, we obtain $T_D = 2 \times 10^4$ orbits, corresponding to 4.3×10^5 yr for $a = 5$ AU.

4.3 Lidov-Kozai effect

In addition to dynamical friction, another mechanism that can affect the orbital evolution of planets on orbits that are highly inclined to the disc is the Lidov-Kozai effect (Kozai 1962). This causes an exchange between inclination and eccentricity for orbits above a critical inclination. Orbits initially with high inclination can thus develop very high eccentricities. For the case of a stationary axisymmetric quadrupole potential, the critical inclination is estimated to be 39° while Terquem & Ajmia (2010) and Teyssandier et al. (2013) find values as small as $\sim 20^\circ$ for a planet interacting with an axisymmetric disc in two and three dimensional treatments respectively. In our case the disc is neither strictly axisymmetric nor steady. However, even though we find that it becomes warped and unsteady from the viewpoint of the planet, the effect remains relatively small so that to a first approximation, the planet may be considered as moving in an axisymmetric potential. However, the component of angular momentum parallel to the symmetry axis will not be strictly conserved, as in that case, giving greater scope for generating inclination changes.

It is important to note that in the axisymmetric case, in the secular theory, a circular orbit at high inclination is on a separatrix (e.g. Funk et al. 2011). Thus it becomes an unstable equilibrium point and chaotic motion is to be expected in its neighbourhood. This raises a potential difficulty in identifying the cause of inclination changes associated with high inclination near circular orbits as being entirely due to frictional effects in simulation runs of limited length. However, we do not see significant eccentricity development, as would be expected if a Lidov-Kozai effect operated in such cases, which indicates that frictional effects are the main cause of the evolution. In addition the characteristic times for evolution can be compared to those expected from dynamical friction and they are found to be comparable.

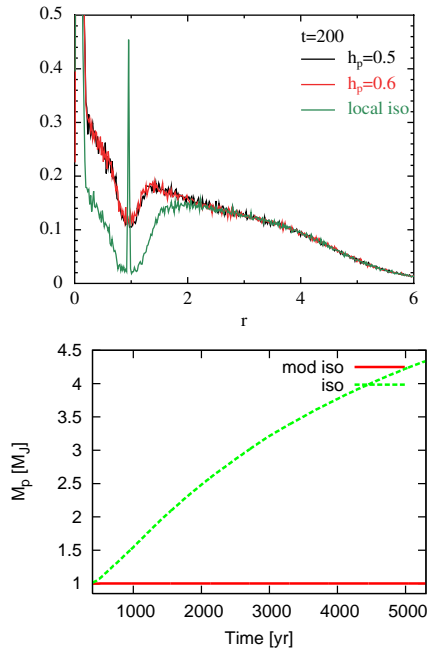


Figure 2. Upper panel: gap formation for $M_p = 1 M_J$ initially with different equations of state, the azimuthally averaged surface density is shown after 200 orbits. The two upper curves corresponding to $h_p = 0.5$ and $h_p = 0.6$ are indistinguishable and the lowest curve is for the locally isothermal equation of state. Lower panel: mass growth starting from an initial planet mass $M_p = 1 M_J$ for $h_p = 0.6$ and locally isothermal equation of state. The upper curve corresponds to the locally isothermal equation of state. There is negligible accretion in the other case.

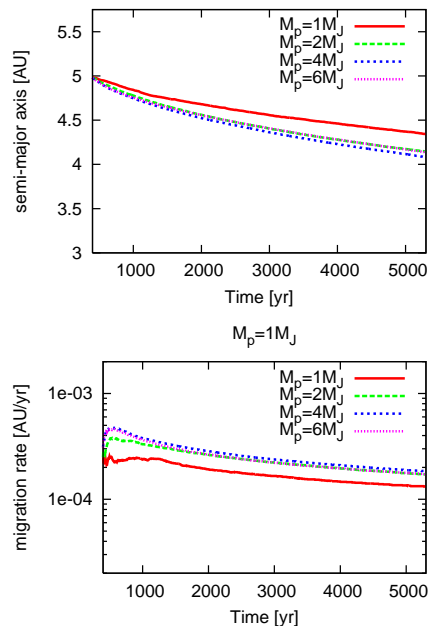


Figure 3. Upper panel: Semi-major axis as a function of time for coplanar planets of different masses (1, 2, 4, 6 M_J). Lower panel: cumulative mean migration rates as a function of time

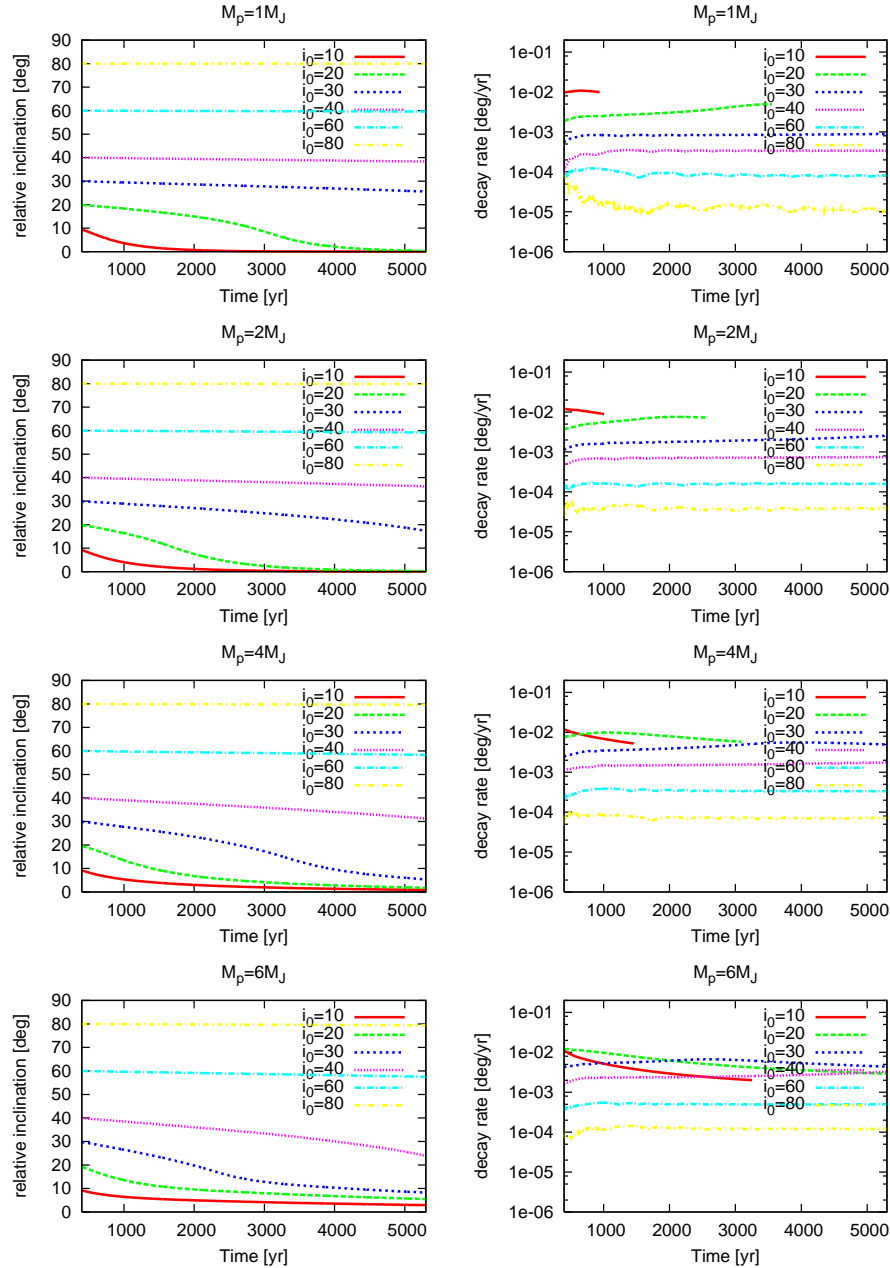


Figure 4. Left: Relative inclination for planet masses (1, 2, 4, 6 M_J) as a function of time. These were initiated on prograde circular orbits with initial relative inclinations 10° , 20° , 30° , 40° , 60° and 80° . Right: Corresponding cumulative means of the relative inclination decay rates as a function of time.

5 NUMERICAL RESULTS WITH A COPLANAR PLANET

In order to understand the orbital evolution of massive planets in the presence of a disc with its total angular momentum vector misaligned with that of the orbit, it is important to consider the extent of the occurrence of gap formation as this would expell material from the neighbourhood of the planets location and so is expected to affect the strength of the interaction of the planet with the disc. This is implied by the simple dynamical friction estimate for the force exerted between the planet and disc given by (10), which indicates that this is proportional to the local disc density. Gap for-

mation is most effective when the planet orbit and disc are coplanar as then the magnitude of the relative velocity between the planet and disc material in its neighbourhood is the smallest. In addition, in contrast to the case of high orbital inclination, the planet then spends most of its time close to disc material. Accordingly, we begin by studying the coplanar case.

5.1 Gap formation in the coplanar case

In this section, we consider the orbital evolution of planets with masses of 1, 2, 4 and 6 M_J initiated in coplanar circular orbits with an initial semi-major axis of 5 AU. Fig.

1 shows the azimuthally averaged disc surface density profile after 200 planet orbits with the modified equation of state. The development of a gap with a depth that increases with planet mass is clearly apparent. The viscous criterion for gap formation given by Lin & Papaloizou (1993) is that $M_p/M_* > 40\alpha_{SS}h_s^2$, where for convenience, we have assumed that the gap extends beyond the region where the modified equation of state changes it from being locally isothermal and that dissipative processes are modelled by a Shakura & Sunyaev (1973) α_{SS} parameterization. For the simulations presented here, this has been estimated to be in the range 0.02 – 0.03 (see appendix B). Thus we should require $M_p/M_* > 0.002 - 0.003$. This is consistent with Fig. 1, which indicates a gap depression of up to 66% for $M_p/M_* = 0.002$ and a deep gap for $M_p/M_* > 0.004$. The 1M_J case is associated with a partial gap associated with a 33% depression of the azimuthally averaged surface density. In addition, we remark that Crida et al. (2006) have studied the gap profile for different viscosities and planet masses. For $M_p = 1$ M_J, they find a gap depth of $\sim 40\%$ for $h_s = 0.05$ and $\alpha_{SS} = 0.025$. We remark that the whole gap width we obtain, in this case being about 0.6 of the orbital radius, is very similar to that found by Crida et al. (2006). Our results are also consistent with those of de Val-Borro et al. (2006) that indicated a somewhat less depleted gap found in SPH simulations as compared to grid based simulations. But note that the treatment of the equation of state and accretion of gas particles differs from ours.

In order to illustrate the effects of the choice of the equation of state on the gap formation process and also the accretion of material by the planet, we illustrate a comparison between runs undertaken with the locally isothermal equation of state and the modified equation of state with $h_p = 0.5$ and $h_p = 0.6$ in Figure 2.

In the locally isothermal case, the planet mass increases to over 4 M_J on a time scale of about five hundred orbits. In this case, a high density of gas particles is able to accumulate in the neighbourhood of the massive planet due to the small effective sound speed around the planet resulting in relatively small pressure forces. Inside the Hill radius, SPH particles build up a hydrostatic equilibrium state with a very high mass density peak centred on the planet. The outer accretion radius is much smaller than the Hill radius in order to prevent any interference with the dynamics on that scale. Therefore, only particles that come very close to the planet can satisfy the conditions to be accreted.

In contrast to the locally isothermal equation of state, the modified equation of state prevents gas particles from accumulating in the vicinity of the planet due to the significantly increased pressure forces occurring because of the increased sound speed. As a consequence, the Hill region around the planet does not contain a high density peak and accretion onto the planet is less significant.

The results for $h_p = 0.5$ and $h_p = 0.6$ are almost identical for the duration of the runs. Values $h_p < 0.5$ were not used for 1 M_J since they result in regions around the planet where the modified $c_{s,mod}$ is smaller than the $c_{s,iso}$ as discussed in appendix A. It can be inferred from this study that the simulations shown in this paper that adopt the modified equation of state do not require implementation of the accretion algorithm. It is nonetheless retained for completeness

and in order to ensure that any potential singularities at the locations of massive particles can be dealt with.

5.2 Migration in the coplanar case

In Fig. 3, the evolution of the semi-major axis a and the migration rate of a coplanar planet are studied. In order to eliminate any effects due to short timescale variations in defining migration rates, we evaluate a cumulative mean of da/dt as

$$\overline{\frac{da}{dt}} = \frac{1}{t} \int_0^t -\frac{da(t')}{dt'} dt' = \frac{a(0) - a(t)}{t}, \quad (15)$$

where $a(t)$ is the semi-major axis at time t and $a(0)$ is its value at $t = 0$. As expected, the migration is always found to be inwards. At the start of the simulations, no gap is present in the disc. During the gap formation phase, the migration rates are largest. At later times, the planets have opened gaps and the migration gradually slows down. The behaviour of the three largest masses is very similar. For $M_p = 1$ M_J, the gap is not as deep as in the other cases resulting in less of a decrease of the migration rate as compared to the other masses. At large times and for gap forming planets that are not too massive compared to the disc mass, inward migration is expected to occur on the viscous timescale of the disc (Lin & Papaloizou 1986). The steady state inflow velocity in a viscous disc is $1.5\alpha_{SS}h_s^2 r_s \Omega_s$ (e.g. Pringle 1981). This leads to an expected migration rate of $3\pi\alpha_{SS}h_s^2/P_{orb}$, where P_{orb} is the local orbital period. For $\alpha_{SS} = 0.025$, this corresponds to 2.5×10^{-4} AU/yr at 5 AU. This is in good agreement with the rates shown at the latest time in Fig. 3 for the three larger masses. For $M_p = 1$ M_J, the migration rate is slightly slower at this time. This may be on account of the differing initial evolution, causing it to be at a larger radius and the presence of more material in the gap region.

6 INTERACTIONS OF PLANETS WITH NON ZERO INCLINATION WITH THE DISC

We now consider the evolution of planets initiated on circular orbits with non zero relative inclination. The relative inclination, i , is defined through

$$i = \arccos\left(\frac{\mathbf{l}_p \cdot \mathbf{L}_D}{|\mathbf{l}_p| \cdot |\mathbf{L}_D|}\right), \quad \text{with} \quad (16)$$

$$\mathbf{L}_D = \sum_i m_i (\mathbf{r}_i \times \mathbf{v}_i). \quad (17)$$

Here \mathbf{l}_p is the angular momentum vector of the planet and \mathbf{L}_D is the total angular momentum vector of the disc, with the summation in (17) being taken over all active gas particles. In simulations starting with circular orbits, the planetary orbit develops only very small eccentricities over their run times. This is in contrast to the situation that occurs when orbits with high enough relative inclination are initiated with a modest non zero eccentricity (see Section 8).

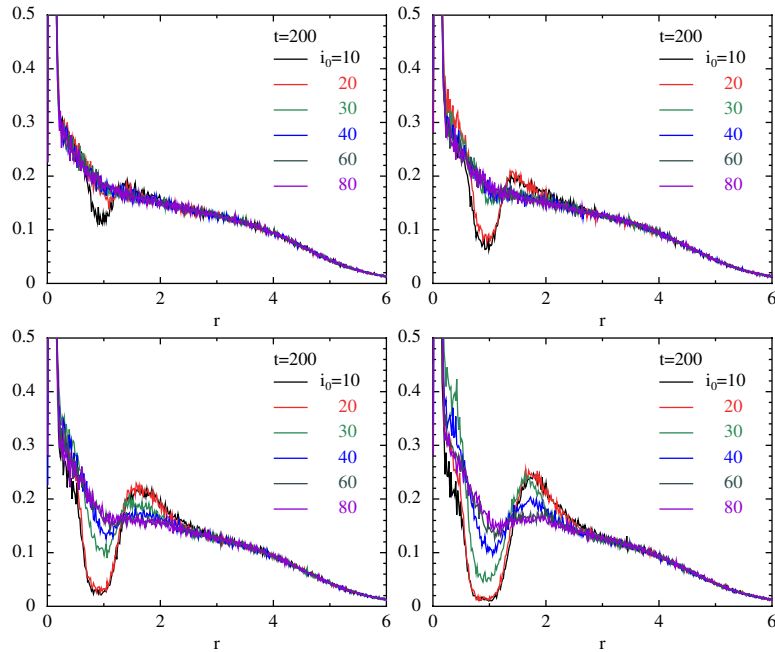


Figure 5. Gap formation for different planet masses and initial relative orbital inclinations: The azimuthally averaged surface density is shown after 200 orbits for, moving from left to right and top to bottom, $M_p = 1, 2, 4$ and $6 M_J$, starting with different initial relative inclinations.

6.1 Decay of the inclination for prograde initially circular orbits

Fig. 4 shows the inclination i of the planet orbit relative to the plane normal to the disc total angular momentum vector and the cumulative mean of its decay rate for planets of mass 1, 2, 4 and 6 M_J initiated on prograde circular orbits with initial relative inclinations $10^\circ, 20^\circ, 30^\circ, 40^\circ, 60^\circ$ and 80° . The cumulative mean of di/dt was adopted in order to iron out small time scale variations. This was defined through

$$\overline{\frac{di}{dt}} = \frac{1}{t} \int_0^t -\frac{di(t')}{dt'} dt' = \frac{i(0) - i(t)}{t}, \quad (18)$$

with $i(t)$ being the relative inclination at time t and $i(0)$ its initial value. This approach loses meaning when the planet becomes almost coplanar with the disc. As can be seen from the left hand panels of Fig. 4, the latter readily happens for $i_0 < 20^\circ$. Cumulative means, defined as above would then approach $i(0)/t$, which is determined by the initial condition. Accordingly decay rates are only shown for relative inclinations above 5° so avoiding this limit.

In general, the cumulative mean of the inclination decay rate decreases in magnitude as the inclination increases. This qualitative feature is consistent with the simplistic estimate of the orbital evolution time scale based on dynamical friction considerations given by (14). This equation suggests that this decay rate should be proportional to $i/(\sin i \sin(i/2)^3)$. Thus comparing the early cumulative mean of the decay rates for $i = 80^\circ$ and $i = 10^\circ$ for 1 M_J in Fig. 4, we find a ratio of $\sim 10^{-3}$, with (14) indicating a ratio of $\sim 3 \times 10^{-3}$. This ratio increases for larger masses on account of gap formation at low inclination. However, in all cases the ratio of the decay rates for $i = 40^\circ$ and $i = 80^\circ$ where gap formation is less relevant is ~ 16 . In this case,

(14) indicates a value of ~ 5 . In view of the very rough nature of the estimate given by (14) the level of agreement is satisfactory.

For $i_0 = 10^\circ$ the results given in Fig. 4 indicate that $T_D \sim 10^3$ yr in the case of 1 M_J while for $i_0 = 80^\circ$, $T_D \sim 10^7$ yr initially. But note that the decay rate accelerates considerably as the inclination decreases so that for $i_0 = 40^\circ$, $T_D \sim 2 \times 10^5$ yr. Again this is in reasonable agreement with the estimate given above derived from equation (14).

For small to intermediate i and larger planet masses, the i -decay is strongly dependent on gap formation, i decreases at an accelerating rate towards smaller values as long as no gap is formed. As soon as i is sufficiently small to open a gap in the disc, the rate of inclination decrease slows down. At large inclinations, the inclination decay rate increases with planet mass so that for $i_0 = 80^\circ$, the decay rate is an order of magnitude faster for 6 M_J as compared to 1 M_J .

6.2 The dependence of gap formation on orbital inclination for prograde orbits

Because the relative velocity between the planet and disc material increases with orbital inclination, the interaction becomes weaker and gap formation is less likely. There can be a threshold inclination above which gap formation does not occur. This threshold inclination for gap opening increases with planet mass. Fig. 5 shows the azimuthally averaged disc surface mass density after 200 orbits for different planet masses and initial inclinations i_0 . We remark that, as can be deduced from the results presented above, after 200 orbits the relative inclination i will have decreased significantly from its initial value i_0 in some cases. For very high inclinations, Σ is marginally perturbed for $M_p = 6 M_J$, the perturbation being weaker for the smaller masses as

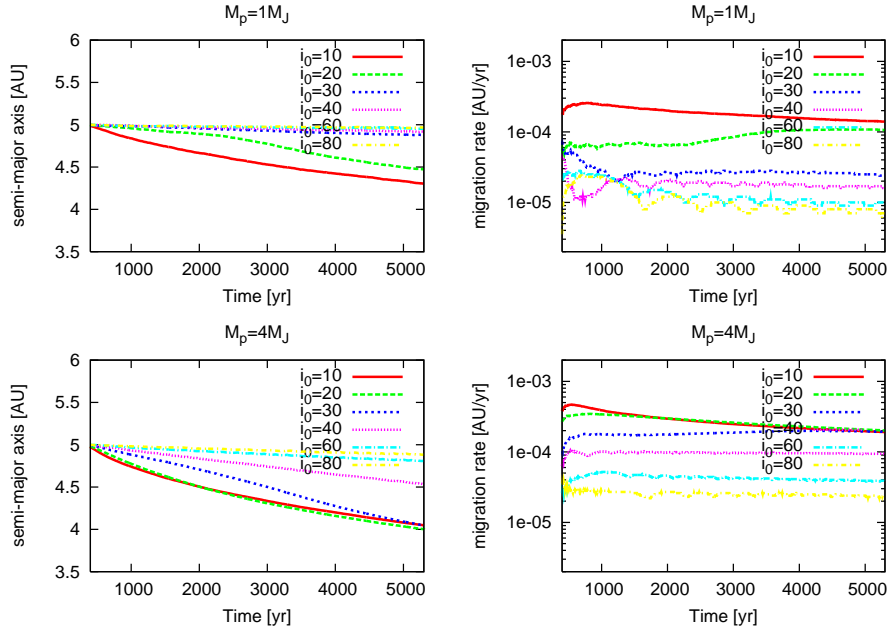


Figure 6. Left: Evolution of the semi-major axis a for planets with $M_p = 1$ and $4 M_J$ for a range of initial relative orbital inclinations, Right: cumulative mean decay rates.

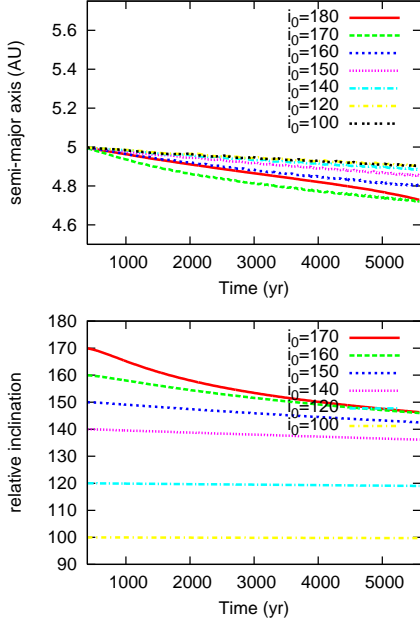


Figure 7. Orbital evolution of a planet with $M_p = 4 M_J$ starting on retrograde circular orbits with different initial relative inclinations. In the upper panel, the semi-major axis is shown as function of time. Lower panel: relative inclination as function of time.

expected. With decreasing i_0 , the interaction between the planet and the disc becomes stronger until eventually the threshold below which a noticeable gap starts to form is passed. Thus for $M_p = 1 M_J$, only the $i_0 = 10^\circ$ curve is able to open a noticeable partial gap. For $M_p = 2 M_J, 4 M_J$ and $6 M_J$, the threshold initial inclinations are $i_0 = 20^\circ, 30^\circ$ and 40° , respectively.

6.3 Evolution of the semi-major axis for finite relative orbital inclination

Fig. 6 shows the evolution of the semi-major axes and cumulative means of the migration rates for planets with $M_p = 1$ and $4 M_J$ initiated on circular orbits with different initial relative orbital inclinations. The cases $M_p = 2$ and $6 M_J$ show very similar behaviour, therefore will not be shown. The runs shown are identical to those illustrated in Fig. 4. Thus corresponding relative inclinations can be read off. As in the coplanar case, the migration is always inwards and the orbits remain almost circular for the run times shown. For planets starting on inclined orbits, the migration rate is slower than for the coplanar case due to the reduced interaction of the planet with the disc. When the relative orbital inclination approaches zero, it is found that the migration rate approaches the value appropriate to coplanar planets. For example, for $M_p = 1 M_J$ and $i_0 = 20^\circ$, i decreases to $< 5^\circ$ after ~ 3000 years. During this time interval, the migration rate approaches the value for a planet of the same mass with $i_0 = 0^\circ$. For $M_p = 4 M_J$ and $i_0 = 30^\circ$, the relative inclination decreases to below 10° for $t > 3000$ yr. At this stage the migration rate approaches that for the coplanar case.

6.4 High inclination retrograde orbits

Finally in this section, we give examples of the orbital evolution of a planet starting on a retrograde circular orbit with varying initial relative orbital inclination. In Fig. 7, we illustrate the evolution of the semi-major axis and the relative orbital inclination as functions of time for a planet of mass $M_p = 4 M_J$. We remark that the direction of evolution of the inclination is always towards coplanarity ($i_{rel} = 0^\circ$), even when the orbit starts out with $i_0 \sim 180^\circ$. This is to be expected from a frictional interaction between the planet and

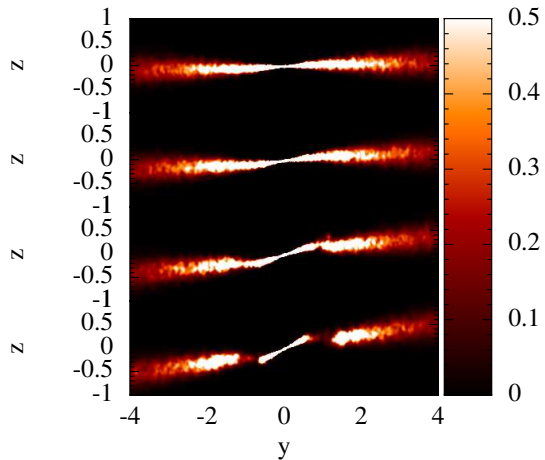


Figure 8. Cross section of the disc as seen in the plane $x = 0$ after 200 orbits, for $M_p = 1, 2, 4$ and $6 M_J$, and $i_0 = 30^\circ$. y and z in units of 5 AU. The orientation of the coordinate system is such that the z axis corresponds to the direction of the angular momentum vector of the initial disc and the planet is initiated at $y = 0$ with $x > 0$ and $z > 0$. [All SPH cross section plots were created using SPLASH (Price 2007)]

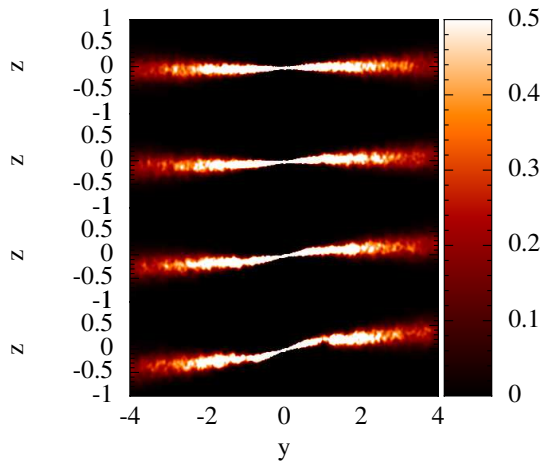


Figure 9. Cross section of the disc as seen in the plane $x = 0$ after 200 orbits, for $M_p = 1, 2, 4$ and $6 M_J$, and $i_0 = 40^\circ$. The coordinate system is as defined in Fig. 8.

the disc which tends to communicate angular momentum in the direction of the disc’s angular momentum vector to the orbit of the planet. In all of these cases, the orbit remains approximately circular. It is seen that the most rapid evolution occurs for the largest inclinations for which the planet tends to become embedded in the disc and thus undergo a more sustained frictional interaction.

7 THE RESPONSE OF THE DISC: INCLINATION CHANGES, WARPING AND PRESSION

As a response to a massive planet, a circumstellar disc can change its orientation significantly, developing a warped structure. So far, we have considered the inclination of the planetary orbits with respect to the plane for which the an-

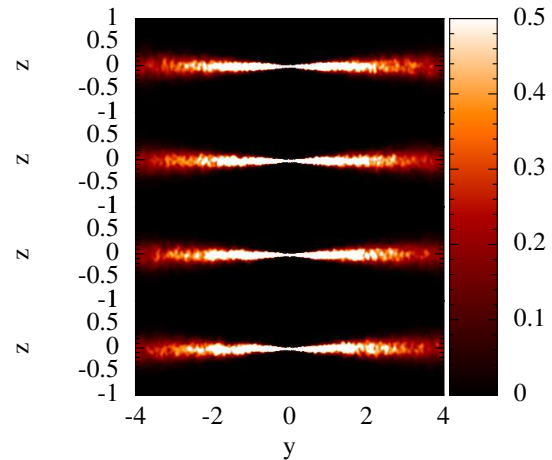


Figure 10. Cross section of the disc as seen in the plane $x = 0$ after 200 orbits, for $M_p = 1, 2, 4$ and $6 M_J$, and $i_0 = 80^\circ$. The coordinate system is as defined in Fig. 8.

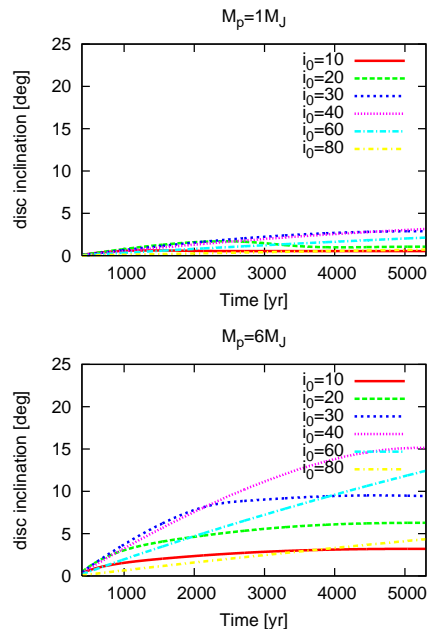


Figure 11. Evolution of total disc inclination for the first 5000 yr for different initial inclinations in the cases $M_p = 1$ and $6 M_J$.

gular momentum vector of the disc as a whole is parallel to the normal. However, warping can be present in the disc, dividing it into two parts with angular momentum vectors pointing in different directions and thus associated with different inclinations. In Figure 8, we show a cross section consisting of the density distribution as seen in the plane $x = 0$ for different planet masses, all of which started with an initial inclination, $i_0 = 30^\circ$, after 200 orbits. This value of i_0 was chosen as maximum warping is expected for an inclination intermediate between 0° and 90° , there being none at these extremes. It is seen that a visible warped inner section of the disc is produced by the more massive planets while planets with $M_p = 1$ and $2 M_J$ do not succeed in creating a visibly warped disc. The same result is found for an initial inclination $i_0 = 40^\circ$ as is illustrated in Fig. 9. The disc pro-

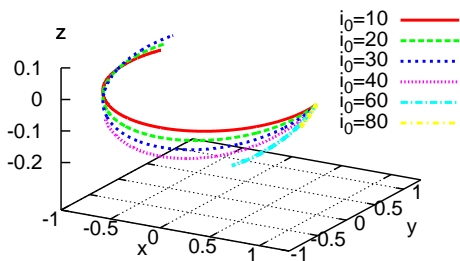


Figure 12. Time-dependent evolution of the unit vector $\mathbf{L}_{D,tot}$ for $M_p = 4 M_J$ and different initial relative inclinations for a period of ~ 5000 years. The coordinate system is as defined in Fig. 8.

M_p [M_J]	i_0 [deg]	i_{rel} [deg]	α_{warp} [deg]
4	30	17.0	10.4
6	30	14.6	19.1
6	40	34.8	10.7

Table 1. Characterising the disc warp: the first column gives the planet mass, the second column the initial relative orbital inclination, the third gives the relative orbital inclination after 200 orbits and the fourth column gives the difference in the inclination angles of the inner and outer disc to the initial disc mid plane.

file is shown for $i_0 = 80^\circ$ for the different planet masses in Fig. 10. In this case no warp is produced since the planets orbit is almost perpendicular to the disc mid plane. An indication of the degree of warping in the above cases can be obtained by measuring the inclination angles between the inner and outer discs as seen in these cross sections. It is noticeable that the inclination of the inner disc can be quite substantial in the direction of aligning with the inclination of the planetary orbit and that this effect is much less severe for the outer disc. Table 1 lists quantities characterising the disc warp after 200 orbits for three runs. As most of the inertia of the disc is in its outer parts, they dominate the inclination of the disc defined by considering its total angular momentum. Fig. 11 shows the evolution of the inclination of the disc, defined in this way, as a function of initial relative inclination of its orbit for the two extreme cases $M_p = 1$ and $M_p = 6 M_J$. By definition the disc inclination is zero at the start of the simulations. The total disc inclination is determined from

$$i_D = \arccos\left(\frac{L_{D,z}}{|\mathbf{L}_D|}\right). \quad (19)$$

In general, the disc inclination based on its total angular momentum does not attain large values in any case because of the high disc inertia. For all the planet masses, the effect of the planet is strongest for the intermediate value $i_0 = 40^\circ$ as expected. Simulations with $i_0 = 60^\circ$ and $i_0 = 80^\circ$ produce lower disc inclinations as would be expected for a rigid planar disc because there would be reduced precessional torques

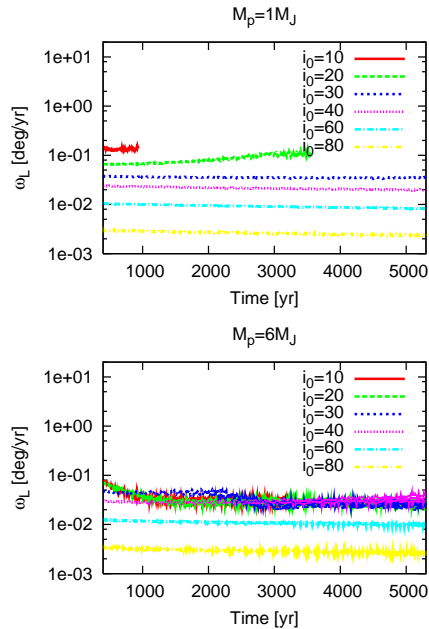


Figure 13. The magnitude of the retrograde precession angular velocity of the disc found from equation (21) as a function of time for planet masses with $M_p = 1$ and $6 M_J$ and various initial relative inclinations.

in those cases. For the highest mass of $6 M_J$, the total disc inclination only attains values up to 15° .

7.1 Disc precession

The gravitational interaction of a disc with a planet in an inclined orbit is expected to make the orbit precess about the total angular momentum vector of the system. Provided communication across the disc through either wave propagation or viscous diffusion occurs more rapidly than the precession rate, the response of the disc would be expected to be to precess like a rigid body in a retrograde sense relative to the orbit (Larwood et al. 1996) while simultaneously undergoing a non disruptive warping. Due to angular momentum conservation of the composite system, this precession is also expected to be about the total angular momentum vector.

In Figure 12, we show the trajectory of the vector $\mathbf{L}_{D,tot}$ defined as

$$\mathbf{L}_{D,tot} = \frac{\mathbf{L}_D \times \mathbf{L}_{tot}}{|\mathbf{L}_D \times \mathbf{L}_{tot}|}. \quad (20)$$

Thus $\mathbf{L}_{D,tot}$ is a unit vector in the direction normal to the plane containing the disc angular momentum, \mathbf{L}_D , and the total angular momentum vector, $\mathbf{L}_{tot} = \mathbf{I}_p + \mathbf{L}_D$, of the system. We focus on the case with $M_p = 4 M_J$, noting that other masses cases manifest similar behaviour. When there is rigid body precession, $\mathbf{L}_{D,tot}$ rotates uniformly with the precession frequency about \mathbf{L}_{tot} also in the retrograde sense. The magnitude of the angular velocity of $\mathbf{L}_{D,tot}$ can be found from

$$\omega_L = \left| \frac{\mathbf{L}_{D,tot} \times \mathbf{v}_L}{|\mathbf{L}_{D,tot}|^2} \right|, \quad (21)$$

where $\mathbf{v}_L = d\mathbf{L}_{D,tot}/dt$. This is shown as a function of time

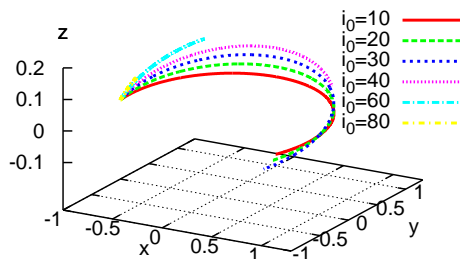


Figure 14. Time-dependent evolution of the precession vector $\mathbf{P}(t)$ for $M_p = 4 M_J$ and different initial inclinations i_0 over ~ 5000 yr. The coordinate system is as defined in Fig. 8.

in Figure 13 for the runs with planet masses $M_p = 1, 6 M_J$ and initial relative orbital inclination. It is found to be almost constant in all cases when a significant relative inclination is present that does not decrease significantly with time, which is a good indication of quasi rigid body precession. It decreases in magnitude as the relative inclination increases which is expected as a reflection of the decrease in magnitude of the precessional torque acting between the planet and the disc as the relative inclination increases.

7.2 Precession of the line of nodes of inclined prograde planet orbits

In addition to the disc precession, the planet orbit also precesses. The orbital angular momentum vector should precess about the total angular momentum vector with the same angular velocity. Figure 14 shows the evolution of the precession vector defined as

$$\mathbf{P} = \frac{\mathbf{l}_p \times \mathbf{L}_{tot}}{|\mathbf{l}_p \times \mathbf{L}_{tot}|} \quad (22)$$

for the case $M_p = 4 M_J$ and different initial inclinations for a time period of ~ 5000 yr. We remark that \mathbf{P} is a unit vector perpendicular to the plane containing the orbital angular momentum vector and the total angular momentum vector. It is found to rotate with the same precession frequency as the disc, as would be expected if the latter precessed like a rigid body. The same behaviour has also been found for all other planet mass cases studied. The precession is retrograde with the inclinations of the plane in which \mathbf{P} evolves being dependent on the initial relative inclination of the planet. The higher the relative initial inclination of the planet orbit, the higher the inclination of the plane of \mathbf{P} . The angular velocity of orbital precession coincides exactly with that of the disc.

8 EVOLUTION OF THE ECCENTRICITY AND THE INDICATION OF A LIDOV-KOZAI EFFECT AT HIGH INCLINATION

So far, we have described simulations for which planets were initiated on circular orbits and in all cases the orbital eccentricity remained very small for the duration of the simulations. However, as the change in inclination of the major-

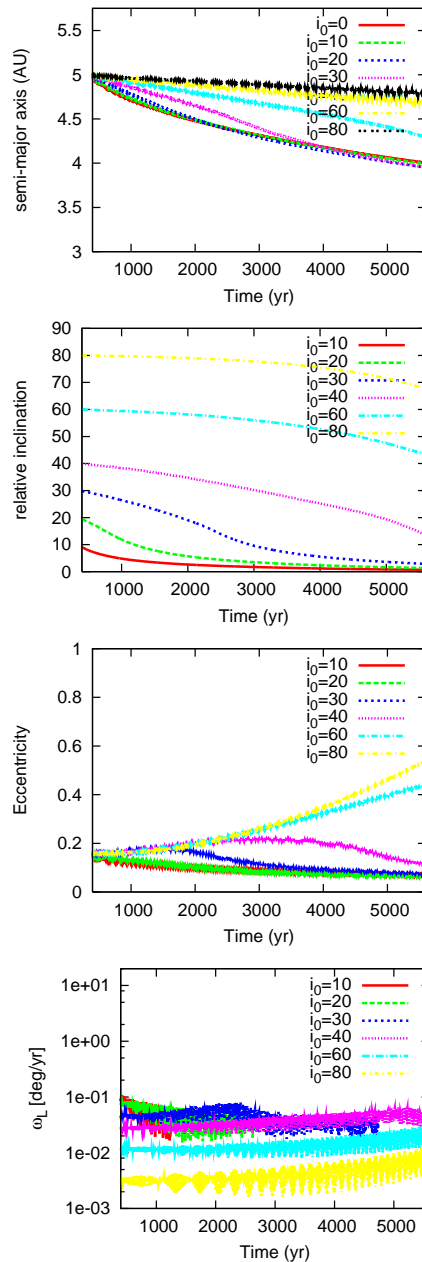


Figure 15. The orbital evolution for a $M_p = 4 M_J$ planet starting on an eccentric orbit with $e = 0.15$ for initial relative orbital inclinations $i_0 = 0^\circ, 10^\circ, 20^\circ, 30^\circ, 40^\circ, 60^\circ$ and 80° .

ity of the disc to the initial mid plane and the corresponding warping distortions are relatively mild, the Lidov-Kozai mechanism applicable to orbits of high inclination with respect to the symmetry plane of an axisymmetric potential might be expected to operate (see the discussion in Section 4.3). As the part of a Lidov-Kozai cycle, where the orbit is nearly circular, corresponds to an extremum of the oscillation and being in the neighbourhood of a separatrix, and our runs were typically less than a precession cycle, development of an exchange between the inclination and eccentricity, characteristic of a Lidov-Kozai cycle, that could take place on longer time scales, may not have been observed. In order to clarify this issue, we initiated runs as before, but

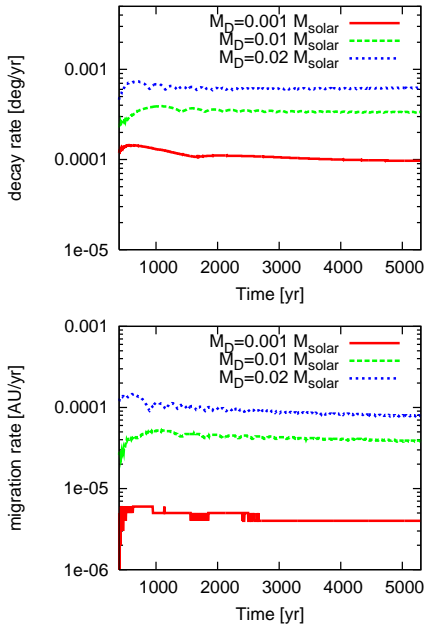


Figure 16. Upper panel: the **cumulative** mean of the relative inclination decay rate for disc masses of 0.001, 0.01 and 0.02 M_{\odot} . Lower panel: as above but for migration rates.

starting with an initial orbital eccentricity of 0.15. In that case, exchange between the inclination and eccentricity is able to occur more rapidly such that it can be seen in our simulations for high masses and high inclinations. We show the results of such simulations for a planet with $M_p = 4 M_J$ starting with different initial relative orbital inclinations in Fig. 15. It is seen that the evolution of the semi-major axis proceeds in almost the same manner as for the cases that started with zero eccentricity. However, in this case we found that although for $i_0 \leq 40^\circ$, the eccentricity ultimately decayed, for the cases of $i_0 = 60^\circ$ and $i_0 = 80^\circ$, significant eccentricities > 0.4 developed and were increasing at the end of the simulations. This was accompanied by a decrease in relative inclination in those cases that was not observed in the cases initiated with circular orbits.

Although these features are suggestive of the operation of a Lidov-Kozai like cycle for $i_0 > \sim 40^\circ$, we remark that the observed decreases in inclination exceeded what would be expected from a conservation of the z component of angular momentum condition that would be applicable for an axisymmetric potential. This could be due to either the operation of dissipative decay and/or non axisymmetric effects. For $i_0 \leq 40^\circ$, the decay rates of the inclinations are about two to three times faster compared to those seen for simulations initiated with circular orbits.

We also ran simulations for a $6 M_J$ planet starting with an initial eccentricity of 0.15 for different initial relative orbital inclinations. Initial inclinations up to 60° show a similar evolution to the $4 M_J$ case. For $i_0 = 80^\circ$, both the inclination decrease and eccentricity increase occur more rapidly. After 5000 years, the relative inclination has decreased to 40° while the eccentricity has reached 0.8. These features are also suggestive of the operation of a Lidov-Kozai like cycle.

The characteristic precession period for initial relative

orbital inclinations $i_0 \leq 60^\circ$ can be extrapolated from Figs. 13 and 15 to be $P_{prec} \sim 3.6 \times 10^4$ yr. This period might also be expected to be comparable to the period of Kozai oscillations. However, the warped structure of the precessing disc may play an important role (see Figs. 8 and 9) leading to modification of the standard description.

8.1 Dependence on the disc mass

So far, all simulations have been carried out for a standard disc mass of $0.01 M_{\odot}$. It is expected that the interaction between planet and disc should increase with disc mass. Simple arguments based on dynamical friction that should be applicable to high inclination cases indicate that decay rates should scale with the disc mass. However, as the planet mass is in general not too different from the disc mass and a considerable amount of non-linearity and some distortion of the shape of the disc is present in our simulations, such a straightforward scaling may not be strictly valid. Figure 16 shows the cumulative mean of relative inclination decay rate for $M_p = 4 M_J$ initiated on a circular orbit with $i_0 = 60^\circ$ for disc masses of 0.001, 0.01, and 0.02 M_{\odot} . The first of these being 10 times smaller than the standard value and the last being twice as large.

It is seen that the migration rates scale as the disc mass as expected from the simple dynamical friction argument. This is also the situation for the inclination decay rate when the larger of the two masses is considered. However, the smallest disc mass has a relative inclination decay rate that is 2 – 2.5 times faster than expected when compared to the standard mass. A closer scrutiny of these cases indicated that the shape of the disc differed in these two cases, with different orientations of the warp. This could result in relatively differing inclination changing torques that could be responsible for this result.

9 CONCLUSIONS

We have performed SPH-simulations in order to undertake a systematic study of the interaction of planets with masses in the range $1 - 6 M_J$ with initial inclinations in the range $[0; 80]^\circ$ with a circumstellar disc. For planets initiated on a coplanar circular orbit gap formation occurred. We found our gap profiles to be consistent with expectations from the work of Lin & Papaloizou (1993) and Crida et al. (2006) for grid based simulations for an adopted viscosity parameter $\alpha_{SS} = 0.025$. Inward migration at a rate of $\sim 2 \times 10^4$ AU/yr for $M_p = 2, 4$ and $6 M_J$ was found and this is in good agreement with previous studies and the theoretical expectation for type II migration. For $M_p = 1 M_J$, which was associated with a partial gap, the migration rate was found to be slightly slower.

We then considered the evolution of planets initiated on the full range of inclined circular orbits. For these simulations, in contrast to those initiated with a finite orbital eccentricity, the orbits remained circular for the duration of the runs. It is possible that phenomena such as the Lidov-Kozai effect did not have time to operate in these cases. The inclination decay rate was found to decrease with increasing inclination and increasing planet mass. This is in full accordance with expectation from estimates based on the

operation of dynamical friction. For a disc mass of $0.01M_{\odot}$, $i_0 = 80^\circ$ and $6 M_J$, the time to decay through 10° was found to be $\sim 10^5$ yr while for $1 M_J$, it is $\sim 10^6$ yr. In the latter case, with the longest decay time, protoplanetary disc lifetimes are approached. For small to intermediate i_0 , gap formation plays a crucial role in the determination of the inclination decay rates. Planets with larger masses are able to form gaps at higher relative inclinations. The reduced amount of material near the planet then causes the frictional interaction to be reduced with a corresponding reduction in the inclination decay rate. After 200 orbits, we find the threshold initial relative inclination below which gap formation starts to occur to be $i_0 = 10^\circ$ for $M_p = 1 M_J$, $i_0 = 20^\circ$ for $M_p = 2 M_J$, $i_0 = 30^\circ$ for $M_p = 4 M_J$ and $i_0 = 40^\circ$ for $M_p = 6 M_J$. For planets on highly inclined orbits, the migration rate was found to be reduced as compared to the coplanar case due to the reduced level of interaction with the disc. When the relative inclination approaches zero, the migration rate approaches that of the coplanar case. For the case of a $4 M_J$ planet initiated on a retrograde circular orbit and different initial inclinations, we found that the direction of evolution tends towards coplanarity ($i = 0^\circ$) as would be expected from interaction with the disc through dynamical friction. The time scale for evolution decreased as i_0 approached 180° . The most extreme case was found for $i_0 = 170^\circ$ where the relative inclination decreased by $\sim 25^\circ$ in ~ 5000 years.

We also found significant changes in the form of the disc that were produced by interaction with the larger planet masses. Visible warping occurred in the inner parts. The difference between the inclinations of the inner and outer part of the disc was found to attain up to $10 - 20^\circ$. Furthermore, we calculated the total disc orientation which can change by up to $\sim 15^\circ$ with respect to its original mid plane. As expected, we also found retrograde precession of both the total disc angular momentum vector and the planet's angular momentum vector about the conserved angular momentum vector of the system. This occurred at an almost constant angular velocity over simulation times, with a magnitude that decreased with increasing relative inclination.

In addition to simulations starting with zero eccentricity, we initiated a $4 M_J$ planet on inclined orbits with $e = 0.15$. While for $i_0 \leq 40^\circ$, the eccentricity decayed, the cases with $i_0 = 60$ and 80° showed an eccentricity increasing for the duration of the simulations. The eccentricity increase was accompanied by a relatively rapid decrease in relative inclination. These characteristics indicate the possibility of a Lidov-Kozai like effect operating in these cases.

In this paper, we have made a first attempt to quantify the possible influences of massive planets with a range of different initial orbital inclinations on a circumstellar disc. Our results are reasonably consistent with theoretical estimates of evolution time scales from dynamical friction, although the simulated behaviour of the disc turns out to be complex in some cases and was not taken into account. In contrast to the situation with low-mass planets, whose influence on a disc is negligible, the results shown in this paper suggest that the interaction of a massive planet with a disc can lead to a strong distortion. Furthermore the stronger frictional interaction is likely to lead to coplanarity within disc lifetimes in most cases. Thus highly inclined orbits are only

likely to survive if they are formed after the disc has mostly dispersed.

ACKNOWLEDGEMENTS

Xiang-Gruess acknowledges support through Leopoldina fellowship programme (fellowship number LPDS 2009-50). Simulations were performed using the Darwin Supercomputer of the University of Cambridge High Performance Computing Service, provided by Dell Inc. using Strategic Research Infrastructure Funding from the Higher Education Funding Council for England and funding from the Science and Technology Facilities Council.

REFERENCES

- Albrecht S., Winn J. N., Johnson J. A., Howard A. W., Marcy G. W., Butler R. P., Arriagada P., Crane J. D., Shectman S. A., Thompson I. B., Hirano T., Bakos G., Hartman J. D., 2012, *ApJ*, 757, 18
- Bate M. R., Bonnell I. A., Price N. M., 1995, *MNRAS*, 277, 362
- Baruteau C., Fromang S., Nelson R. P., Masset F., 2011, *A&A*, 533, A84
- Bate M. R., Lodato G., Pringle J.E., 2010, *MNRAS*, 401, 1505
- Bitsch B. & Kley W., 2011, *A&A*, 530, A41
- Cresswell P., Dirksen G., Kley W., Nelson R. P., 2007, *A&A*, 473, 329
- Crida A., Morbidelli A., Masset F., 2006, *Icarus*, 181, 587
- Dawson R. I., Murray-Clay R. A., Johnson J. A., 2012, *arXiv:1211.0554*
- de Val-Borro M. et al., 2006, *MNRAS*, 370, 529
- Fabrycky D. & Termain S., 2007, *ApJ*, 669, 1298
- Ford E. B., Kozinsky B., Rasio F. A., 2000, *ApJ*, 535, 385
- Fragner M. M. & Nelson R. P., 2010, *A&A*, 511, A77
- Funk B., Libert A.-S., Süli Á., Pilat-Lohinger E., 2011, *A&A*, 526, 98
- Kley W. & Nelson R. P., 2012, *ARA&A*, 50, 211
- Kozai Y., 1962, *AJ*, 67, 591
- Lai D., Foucart F., Lin D. N. C., 2011, *MNRAS*, 412, 2790
- Larwood J. D., Nelson R. P., Papaloizou J. C. B., Terquem C., 1996, *MNRAS*, 282, 597
- Lin D. N. C. & Papaloizou J. C. P., 1979, *MNRAS*, 186, 799
- Lin D. N. C. & Papaloizou J. C. P., 1986, *ApJ*, 309, 846
- Lin D. N. C. & Papaloizou J. C. P., 1993, *Protostars and planets III*, (A93-42937 17-90), 749-835
- Marzari F. & Nelson A. F., 2009, *ApJ*, 705, 1575
- Mayer L., Quinn T., Wadsley J., Stadel J., 2002, *Science*, 298, 1756
- Mizuno H., 1980, *Progress of Theoretical Physics*, 64, 544
- Nagasawa M., Ida S., Bessho T., 2008, *ApJ*, 678, 498
- Nelson R. P. & Papaloizou J. C. B., 2003, *MNRAS*, 339, 993
- Ostriker E. C., 1999, *ApJ*, 513, 252
- Papaloizou J. C. B., Larwood J. D., 2000, *MNRAS*, 315, 823
- Papaloizou J. C. B. & Terquem C., 2001, *MNRAS*, 325, 221

- Papaloizou J. C. B., Nelson R. P., Kley W., Masset F. S., Artymowicz P., 2007, *Protostars and Planets V.*, Univ. Arizona Press, Tucson, AZ, p. 655
- Peplinski A., Artymowicz P., Mellema G., 2008, *MNRAS*, 386, 164
- Pollack J. B., Hubickyj, O., Bodenheimer P., Lissauer J. J., Podolak M., Greenzweig Y., 1996, *Icarus*, 124, 62
- Price D., 2007, *Proc. Astron. Soc. Aust.*, 24, 159
- Pringle J. E., 1981, *ARA&A*, 19, 137
- Rasio F. A. & Ford E. B., 1996, *Science*, 274, 954
- Rein H, 2012, *MNRAS*, 422, 3611
- Rephaeli Y. & Salpeter E. E., 1980, *ApJ*, 240, 20R
- Rudermann M. A. & Spiegel E. A., 1971, *ApJ*, 165, 1R
- Shakura N. I. & Sunyaev R. A., 1973, *A & A*, 24, 337
- Schäfer C., Speith R., Hipp M., Kley W., 2004, *A&A*, 418, 325
- Speith R. & Kley W., 2003, *A&A*, 399, 395
- Speith R., Riffert H., 1999, *Journal of Computational and Applied Mathematics*, 109, 231
- Springel V. , 2005, *MNRAS*, 364, 1105
- Terquem C., Ajmia A., 2010, *MNRAS*, 404, 409
- Teyssandier J., Terquem C., Papaloizou J. C. B., 2013, *MNRAS*, 428, 658
- Thommes , Lissauer, 2003, *ApJ*, 597, 566
- Thies I., Kroupa P., Goodwin S. P., Stamatellos D., Whitworth A. P., 2011, *MNRAS*, 417, 1817
- Triaud A. H. M. J. et al., 2010, *A& A*, 524, A25
- Varnière P., Quillen A.C., Frank A., 2004, *ApJ*, 612, 1152
- Watson C. A., Littlefair S. P., Diamond C., Collier Cameron A., Fitzsimmons A., Simpson E., Moulds V., Pollacco D., 2011, *MNRAS*, 413, L71
- Weidenschilling S. J. & Marzari F., 1996, *Nature*, 384, 619
- Wu Y., Murray N. W., Ramsahai J. M., 2007, *ApJ*, 670, 820

APPENDIX A: CHOICE OF ASPECT RATIO IN THE CIRCUMPLANETARY DISC FOR THE MODIFIED EQUATION OF STATE

The main motivation of Peplinski et al. (2008) is to introduce a modification to the locally isothermal equation of state in order to prevent a large amount of gas from being accreted by massive planets. In the close vicinity of massive planets, the sound speed is enhanced, as would be expected for accreted optically thick material in hydrostatic equilibrium. This feature is not described by a locally isothermal equation of state. Thus the modified sound speed $c_{s,mod}$ is designed to be the sum of the unmodified soundspeed $c_{s,iso}$ and an additional positive quantity whose value increases towards the planet and tends to zero far from it.

Given the motivation indicated above, $c_{s,mod}$ should be everywhere larger than $c_{s,iso}$. Peplinski et al. (2008) have shown through various tests with planets with mass exceeding $1M_J$, that $h_p \leq 0.4$ is appropriate in order to prevent large amounts of gas from being accreted. Our studies have shown that for a given planet mass, M_p , there exists a lower limit $h_{p,lim}$ which must be exceeded in order to guarantee that $c_{s,mod} \geq c_{s,iso}$ globally. For $h_p \leq h_{p,lim}$, $c_{s,mod} \leq c_{s,iso}$ somewhere and the modification does not comply with physical requirements. In Table A1, some values of $h_{p,lim}$ are listed. The lower bound $h_{p,lim}$ decreases with

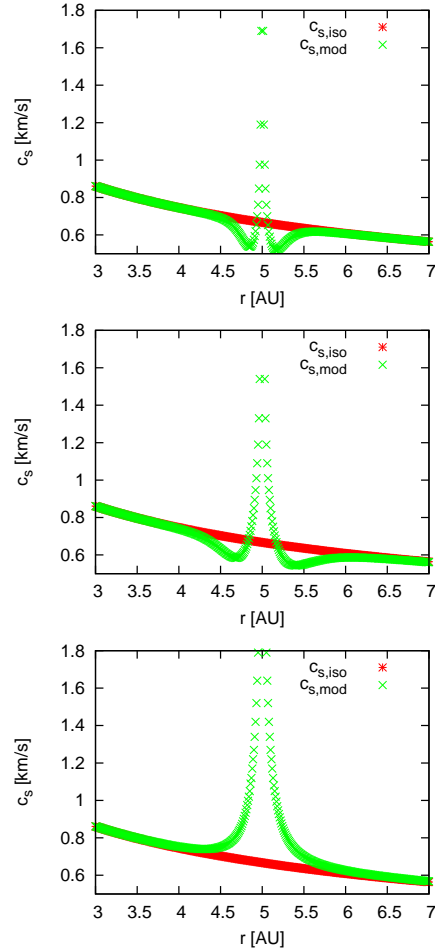


Figure A1. Modified sound speed and locally isothermal sound speed for $M_p = 0.1 M_J$, $h_p = 0.8$ (top); $M_p = 1 M_J$, $h_p = 0.4$ (middle); $M_p = 1 M_J$, $h_p = 0.6$ (bottom).

M_p [M_J]	0.1	0.2	0.5	1	2	4	6
$h_{p,lim}$	1.06	0.84	0.62	0.49	0.39	0.31	0.27

Table A1. Lower bounds $h_{p,lim}$ for different planet masses

increasing planet mass. For $1 M_J$, we suggest $h_p > 0.49$ for the above reasons. Fig. A1 illustrates two examples where $c_{s,mod} < c_{s,iso}$ and a third that achieves a successful modification of the equation of state.

APPENDIX B: RING SPREADING TEST

The spreading of a viscous gas ring is often used to calibrate the effective viscosity (e.g. Speith & Riffert 1999). The analytic solution describing an axisymmetric thin disc of gas moving around a central point mass M_c under gravity and viscous stresses is considered. The vertical scale height, H , of the disc is assumed to be negligible compared to the radial length scale and the viscous time scale governing the radial inflow of mass is assumed to be much larger than the dynamical time scale. In the thin-disc approximation, it is possible to integrate the governing equations over the height

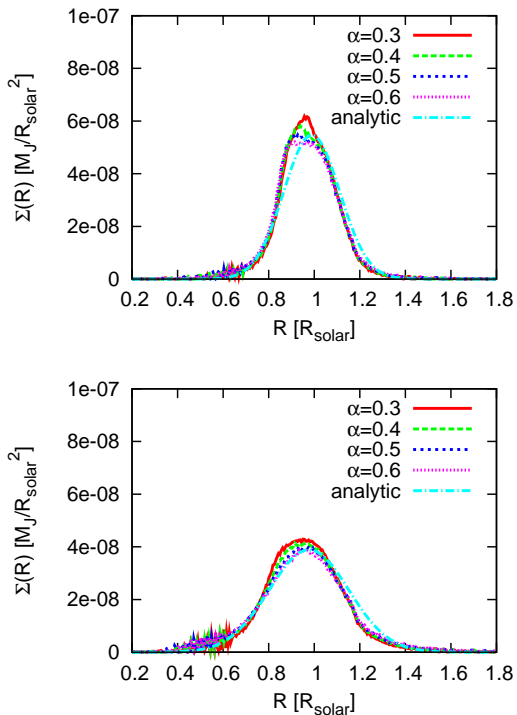


Figure B1. Comparison between the analytical and numerical solutions with different values for the artificial viscosity parameter α (see Section 2.2) as indicated.

of the disc and consider a two dimensional flow. Adopting polar coordinates (R, φ) , there are two velocity components (v_R, v_φ) , and the mass distribution is described by the surface density

$$\Sigma(R, t) = \int_{-\infty}^{+\infty} \rho dz, \quad (\text{B1})$$

where ρ is the mass density. Assuming that the radial inflow of mass is caused entirely by viscous stresses, the surface density can be shown to satisfy the diffusion equation (Pringle 1981)

$$\frac{\partial \Sigma}{\partial t} = \frac{3}{R} \frac{\partial}{\partial R} \left[\sqrt{R} \frac{\partial}{\partial R} (\nu_0 \sqrt{R} \Sigma) \right]. \quad (\text{B2})$$

If the initial surface density distribution is chosen to be proportional to a δ function corresponding to a ring of mass M localised at an initial radius R_0 , then the initial surface density distribution $\Sigma_0(R)$ is given by

$$\Sigma_0(R) = \frac{M}{2\pi R_0} \delta(R - R_0) \quad (\text{B3})$$

The analytic solution of (B2) gives Σ at a later time as

$$\Sigma(R, t) = \frac{M}{\pi R_0^2} \frac{1}{\tau x^{1/4}} I_{1/4} \left(\frac{2x}{\tau} \right) \exp \left(-\frac{1+x^2}{\tau} \right), \quad (\text{B4})$$

$$\text{with } v_R = \frac{6\nu_0}{R_0 \tau} \left[x - I_{-3/4} \left(\frac{2x}{\tau} \right) / I_{1/4} \left(\frac{2x}{\tau} \right) \right]. \quad (\text{B5})$$

Here I are the modified Bessel functions. $x = R/R_0$, $\tau = 12\nu_0 t/R_0^2$ is the time in units of the viscous time scale $R_0^2/(12\nu_0)$ and ν_0 is the kinematic viscosity (see Pringle 1981). We adopt the values $R_0 = 1 R_\odot$, $M = 10^{-10} M_\odot$,

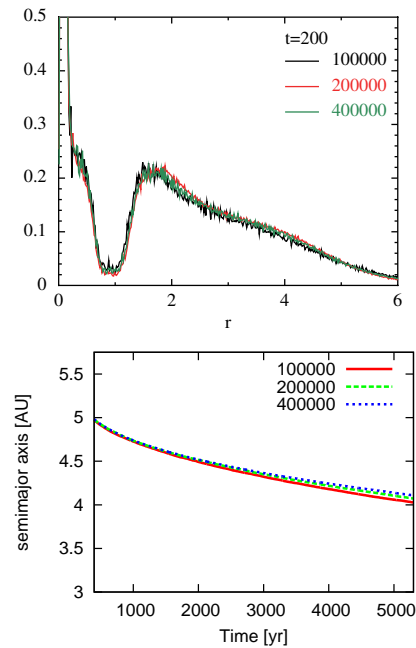


Figure C1. Resolution study of gap formation (upper panel) and corresponding migration (lower panel) for a coplanar planet with $M_p = 4 M_J$ and a disc of $M_D = 0.01 M_\odot$. Curves corresponding to runs with different numbers of particles as indicated.

$M_c = 1 M_\odot$, $\nu_0 = 1.5 \cdot 10^{14} \text{ cm}^2/\text{s}$ (see also Speith & Kley (2003)). Since $\Sigma(t=0)$ is a δ -function, the test is started by initiating the state variables to match conditions at $\tau = 0.02$ and then the system is evolved forwards in time. The corresponding dimensionless α_{SS} parameter (Shakura & Sunyaev 1973) corresponding to this optimised value of ν_0 is

$$\alpha_{SS} = \frac{\nu_0}{c_s H} = \frac{1.5 \cdot 10^{14} \text{ cm}^2/\text{s}}{0.05^2 \sqrt{GM_\odot R_\odot}} = 0.0196 \cong 0.02. \quad (\text{B6})$$

Results from our test calculations with 2×10^5 SPH particles, are shown in Figure B1. In contrast to Speith & Kley (2003), we didn't find any indications for spiral arm formation. In this context we note that according to these authors, the spiral features are associated with instabilities driven by shear viscosity and that they used a version of SPH with a treatment of viscosity that differs from the one we used.

APPENDIX C: RESOLUTION STUDY

In order to investigate the sensitivity of the simulations to the number of SPH particles used, we have performed a number of studies with differing numbers of particles for a planet with $M_p = 4 M_J$ initiated on both circular orbits, and orbits with an initial eccentricity, around a central star with $M_* = 1 M_\odot$ and interacting with a disc with $M_D = 0.01 M_\odot$. We considered the coplanar case, $i_0 = 0$, and the case where $i_0 = 60^\circ$.

Runs were performed with, 10^5 , 2×10^5 , and 4×10^5 SPH particles. We remark that as shown by ring spreading tests, a disc modelled with SPH particles has a non zero effective shear viscosity that is expected to decrease weakly as the number of particles is increased. Thus one wants to verify that a fluid disc with an effective shear viscosity is

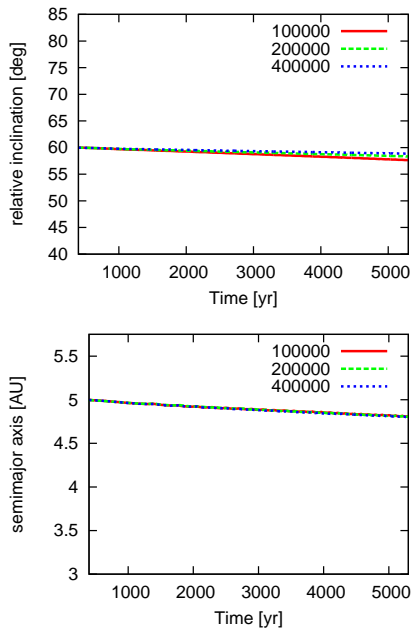


Figure C2. Resolution study of relative inclination evolution (upper panel) and inward migration (lower panel) for a planet with $M_p = 4 M_J$ and $i_0 = 60^\circ$. The disc mass was $M_D = 0.01 M_\odot$. Curves corresponding to runs with different numbers of particles as indicated.

appropriately modelled for the number of particles chosen. For all these test studies, the disc was allowed to evolve for 30 orbits without the planet in order to allow any initial inhomogeneities and fluctuations to be smoothed out. The planet was then suddenly introduced after 30 orbits. The sudden introduction produces transients that rapidly decay and so produce no lasting noticeable effects.

In Fig. C1 we show the results for initiation on a circular orbit with $i_0 = 0$. Gap profiles and the evolution of the semi-major axis are plotted for the three runs with differing numbers of SPH particles. For both gap profiles and the evolution of the semi-major axis, the different resolution levels show good agreement over the run time of the simulations. There is a hint of a decreasing shear viscosity with increasing numbers of particles, as the semi-major axis decreases slightly less, but this effect is small.

Fig. C2 shows the evolution of the relative inclination and the semi-major axis for the cases when the planet is initiated on a circular orbit with $i_0 = 60^\circ$. The results of simulations carried out with different numbers of particles are also seen to be in good agreement. In this case the evolution is expected to be driven by dynamical friction and thus expected to be insensitive to disc viscosity. The evolution of the semi-major axis is indistinguishable in these cases. The correspondence for the evolution of the relative inclination is not quite as precise. However, note that the evolution of the relative inclination is particularly sensitive because the initial orbit is likely to be close to a separatrix and its initial evolution thus expected to be sensitive to small perturbations (see discussion in Section 4.3).

We have also run a resolution test for a planet starting with $i_0 = 60^\circ$ and an initial eccentricity $e \cong 0.15$. This study was performed to check the results described in Section 8.

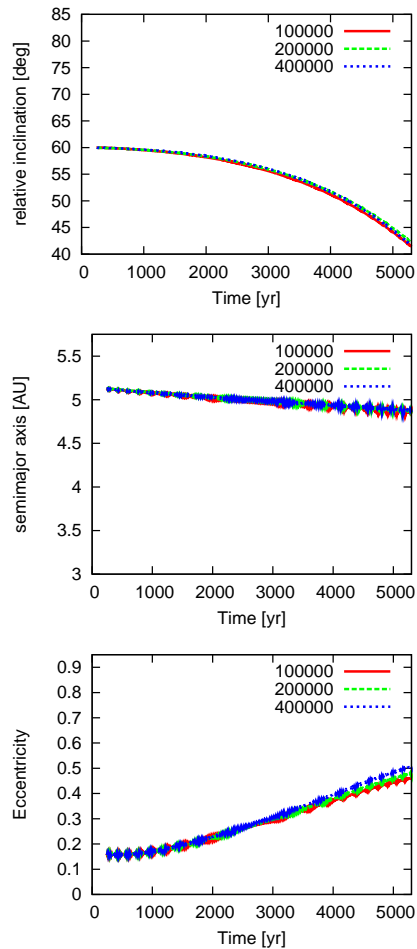


Figure C3. Top two panels: as for Fig. C2 but starting with an initial eccentricity of 0.15. Bottom panel: The evolution of the eccentricity is shown.

The evolution is again expected to be controlled by dynamical friction and insensitive to disc viscosity. The inclination and semi-major axis evolution are plotted in Fig. C3. The results of simulations carried out with different numbers of particles are seen to be in good agreement. The runs undertaken with different numbers of particles thus indicate good convergence and that a choice of 2×10^5 SPH particles for simulations of the type presented here is a reasonable one.

This paper has been typeset from a $\text{\TeX}/\text{\LaTeX}$ file prepared by the author.